Title

Ruthenium-Catalyzed Asymmetric Hydrohydroxyalkylation of Butadiene: The Role of the Formyl Hydrogen Bond in Stereochemical Control

Journal

Journal of the American Chemical Society, 137(27)

ISSN

0002-7863

Authors

Grayson, Matthew N
Krische, Michael J
Houk, KN

Publication Date

2015-07-15

DOI

10.1021/jacs.5b04844

Peer reviewed

HHS Public Access

Author manuscript

J Am Chem Soc. Author manuscript; available in PMC 2016 July 15.

Published in final edited form as:

J Am Chem Soc. 2015 July 15; 137(27): 8838–8850. doi:10.1021/jacs.5b04844.

Ruthenium-Catalyzed Asymmetric Hydrohydroxyalkylation of Butadiene: The Role of the Formyl Hydrogen Bond in Stereochemical Control

Matthew N. Grayson[†], **Michael J. Krische**[‡], and **K. N. Houk**[†,*]

[†]Department of Chemistry and Biochemistry, University of California, Los Angeles, California 90095-1569, United States

[‡]Department of Chemistry and Biochemistry, University of Texas at Austin, Austin, Texas 78712, United States

Abstract

The catalyst generated in situ from $RuH_2(CO)(PPh_3)_3$, (*S*)-SEGPHOS, and a chiral phosphoric acid promotes asymmetric hydrohydroxyalkylation of butadiene and affords enantioenriched α-methyl homoallylic alcohols. The observed diastereo- and enantioselectivities are determined by both the chiral phosphine and chiral phosphate ligands. Density functional theory calculations (M06/SDD-6-311G(d,p)-IEFPCM(acetone)//B3LYP/SDD-6-31G(d)) predict that the product distribution is controlled by the kinetics of carbon-carbon bond formation, and this process occurs via a closed-chair Zimmerman-Traxler-type transition structure (TS). Chiral phosphate-dependent stereoselectivity arising from this TS is enabled through a hydrogen bond between the phosphoryl oxygen and the aldehyde formyl proton present in TADDOL-derived catalysts. This interaction is absent in the corresponding BINOL-derived systems and the opposite sense of attack on the aldehyde occurs. Additional factors influencing stereochemical control are determined.

1. INTRODUCTION

The introduction of crotyl (α-methylallyl) groups into organic molecules is an important type of stereoselective carbon-carbon bond formation.[1,2] The crotylation of carbonyl compounds introduces multiple stereogenic centers, and the double bond of the resulting α-methyl homoallylic alcohol is a useful synthetic handle.[3] This type of reaction has been used extensively in natural product synthesis.[4] Many different asymmetric methods exist to synthesize α-methyl homoallylic alcohols, but these typically rely upon either substrate or reagent control.[5,6] The crotylboration of aldehydes is a typical example (Scheme 1).

Krische's ruthenium-catalyzed asymmetric hydrohydroxyalkylation of butadiene is an alternate strategy for the crotylation of carbonyl compounds. It has the advantage of

[*]**Corresponding Author**. houk@chem.ucla.edu.

ASSOCIATED CONTENT

Supporting Information. Complete list of authors in the Gaussian09 reference; Cartesian coordinates, energies and number of imaginary frequencies of all stationary points and values of imaginary frequencies of all transition structures. This material is available free of charge via the Internet at http://pubs.acs.org

bypassing the use of chiral pre-metallated reagents. The catalyst generated in situ from $RuH_2(CO)(PPh_3)_3$, dppf, and a BINOL-derived phosphoric acid promotes asymmetric hydrohydroxyalkylation of butadiene and affords enantioenriched α-methyl homoallylic alcohols with good levels of *anti*-diastereoselectivity (Scheme 2).[9] Furthermore, by using the catalyst system derived from $RuH_2(CO)(PPh_3)_3$, (*S*)-SEGPHOS and a chiral phosphoric acid, the diastereoselectivity can be controlled by changing the chiral phosphoric acid (Scheme 3).[10] Catalyst systems generated from TADDOL-derived phosphate ligand **1a** delivered α-methyl homoallylic alcohols with good levels of *syn*-diastereoselectivity and high levels of enantioselectivity. Match/mismatch effects between the chiral phosphate ligand **1b** and the chiral phosphine ligands (*R*)- and (*S*)-SEGPHOS also impact upon enantioselectivity (vide infra). Catalyst systems generated from BINOL-derived phosphate **2a** led to *anti*-diastereoselectivity and attack on the opposite face of the prochiral aldehyde. The origins of this unexpected chiral phosphate-dependent stereoselectivity were unknown, but are the subject of the computational investigation reported here.

Scheme 4 shows the proposed catalytic cycle for ruthenium-catalyzed asymmetric hydrohydroxyalkylation of butadiene.[9,10] A computational study of an achiral, iridium-catalyzed process by Li and Wang supports this cycle.[11] As shown in Scheme 4, *syn*-π- and *anti*-π-crotylruthenium isomers yield the (*E*)- and (*Z*)-σ-crotylruthenium species respectively. The π-allyl species can isomerize through an η^3-η^1-η^3 type process (π-σ-π allyl isomerization).[12,13] Given a rapidly interconverting mixture of π-allyl species, C-C bond formation via a closed-chair Zimmerman-Traxler-type transition structure (TS) is expected to yield a*nti*-diastereoselectivity as a result of preferential reaction of the (*E*)-σ isomer which places both methyl group and aldehyde substituent equatorial in the TS.[14] Therefore, the unexpected *syn*-diastereoselectivity observed with TADDOL-derived phosphates was suggested to arise from slow isomerization between π-crotylruthenium isomers. Such a mechanism would deliver exclusively the (*Z*)-σ-crotylruthenium isomer from the *anti*-π-crotylruthenium species after the kinetically preferred hydrometalation of the s-*cis* conformer of butadiene.[10]

However, experimental evidence suggests this isomerization is rapid under the reaction conditions, and that the final product distribution is controlled by the kinetics of C-C bond formation.[15–17] After C-C bond formation, the resulting homoallylic ruthenium alkoxide exchanges with a reactant alcohol to release the product. The catalytic cycle is closed by dehydrogenation to form the aldehyde and regenerate the ruthenium hydride.[9]

We have carried out density functional theory (DFT) calculations that show that the product distribution is controlled by the kinetics of carbon-carbon bond formation. This process occurs via a closed-chair Zimmerman-Traxler-type TS. Chiral phosphate-dependent stereoselectivity arising from this TS is influenced by a hydrogen bond between the phosphoryl oxygen and the aldehyde formyl proton present in TADDOL-derived catalysts. This hydrogen bond is absent in the corresponding BINOL-derived systems due to a steric clash between the chiral phosphine and chiral phosphate ligands. Additional factors influencing stereochemical control are determined. Match/mismatch effects between the chiral phosphate ligand **1b** and the chiral phosphine ligands (*R*)- and (*S*)-SEGPHOS are qualitatively rationalized.

2. COMPUTATIONAL DETAILS

Quantum mechanical calculations were performed using Gaussian09 (Revision D.01).[18] All geometries were optimized using the B3LYP density functional,[19,20] and the SDD basis set for ruthenium and 6-31G(d) for all other atoms. Single point energies were calculated using M06,[21] within the IEFPCM model (acetone),[22] and with a mixed basis set of SDD for ruthenium and 6-311G(d,p) for all other atoms. The resulting energies were used to correct the gas phase energies obtained from the B3LYP calculations.[23–25] Previous computational studies of ruthenium catalysts with these methods provided results in accord with experiment.[26–28] Computed structures are illustrated with CYLView.[29]

The arrangements of ligands around ruthenium and conformation of the phosphate ligand in our calculations are derived from the X-ray crystal structure of a TADDOL-derived catalyst system reported by Krische and co-workers.[10] The chiral phosphates were truncated as outlined in Scheme 3 to simplify our calculations (**1b** and **2b**). Both of these truncated phosphates were tested experimentally under unoptimized conditions and were reported to have minimal effect on the reaction outcome (**1a** = 94% ee, 4.1:1 dr, **1b** = 90% ee, 3.0:1 dr[10]; **2a** = 72% ee, 4:1 dr, **2b** = 72% ee, 5:1 dr[9]). The aldehydes were also truncated to ethanal.[30]

3. RESULTS AND DISCUSSION

TADDOL-derived catalyst system

The orientation of the SEGPHOS phenyl groups are controlled by the ligand's C_2-symmetric nature (Figure 1a). The TADDOL framework adopts a "slanted" orientation with respect to the P-Ru-P plane which makes interactions with the left-hand side phenyl groups of SEGPHOS the most important (Figure 1b). The left, upwards pointing phenyl group of SEGPHOS occupies an empty quadrant of the TADDOL-derived scaffold helping to restrict phosphate rotation (Figure 1c). The slanted nature of the phosphate also creates a network of CH-π interactions between the TADDOL-derived phosphate and the left-hand side phenyl groups of SEGPHOS which increases the conformational rigidity of the catalyst structure (Figure 1d). Therefore, the chirality of the two ligands complement each other which leads to a well-defined chiral pocket in the empty quadrant in which carbonyl crotylation can occur. (*R*)-SEGPHOS leads to lower enantioselectivity under unoptimized conditions ((*S*)-SEGPHOS = 89% ee, (*R*)-SEGPHOS = 31% ee). Qualitatively, this is expected to be the result of reduced catalyst conformational rigidity due to a mismatch between the SEGPHOS phenyl groups, which are now the mirror image of Figure 1a, and the slanted nature of the chiral phosphate which disrupts the CH-π interactions and the intersection of the upwards pointing phenyl group of SEGPHOS with the TADDOL-derived scaffold. In the presence of an achiral phosphine (dppf), modest enantioselectivity is observed under unoptimized conditions ((*S*)-SEGPHOS = 89% ee, dppf = 78% ee). In the absence of a rigid chiral ligand, the resulting increase in phosphine conformational flexibility is expected to lead to fluxional matching and mismatching between the phosphine and the TADDOL-derived framework and hence lower enantioselectivity.

The π-allyl species are expected to be, or close in energy to, the resting state of the catalytic cycle.[11] To gain an insight into their structures, all 8 possible π-allyl species were located. These arise from the following variables: π-crotylruthenium isomer (*syn* or *anti*) and α-methyl group orientation (toward or away from phosphate, and left or right). For reaction (1) (Scheme 3), DFT calculations show that the thermodynamically preferred π-crotylruthenium isomer is the *syn*-π-allyl species by 6.4 kcal mol^{-1} (Figure 2). However, as described above, these π-allyl species are in rapid equilibrium and that their relative thermodynamic stabilities do not determine diastereocontrol (Curtin-Hammett conditions).[31] Therefore, the kinetics of C-C bond formation were investigated.

All 16 possible chair-like C-C bond forming TSs were located for reaction (1). These arise from the following variables: σ-crotylruthenium isomer (*E* or *Z*), aldehyde substituent orientation (toward or away from phosphate, and axial or equatorial) and aldehyde coordination site (site 1 or 2, Scheme 4). All 4 (*Z*)-σ-crotylruthenium boat-like C-C bond forming TSs with aldehyde substituent equatorial were calculated to be strongly disfavored relative to the lowest energy chair-like TS (over 5 kcal mol^{-1}). Therefore, boat-like TSs were not investigated further. TSs with alternative P=O orientations leading to the major product were also explored but were calculated to be strongly disfavored relative to the TS in which the P=O is orientated over the substrate (over 4 kcal mol^{-1}). Twenty-four unique TS were found in total. The four lowest energy TSs which led to each of the experimentally observed products are shown below in Figure 3 and Table 1.

The lowest energy TS, **TS-1(3*R*,4*R*)** leads to the major product observed experimentally. From the lowest energy *syn*-π-allyl species, the barrier to this TS is 24.3 kcal mol^{-1}. In both **TS-1(3*R*,4*R*)** and **TS-1(3*S*,4*R*)**, there is a hydrogen-bonding interaction from the catalyst phosphoryl oxygen to the aldehyde formyl proton. The formyl hydrogen bond has previously been identified as playing a crucial role in phosphoric acid catalyzed asymmetric aldehyde allylboration and allenylboration, and in these reactions this interaction is calculated to be worth approximately 3 kcal mol^{-1}.[32,33] The H…O distances in **TS-1(3*R*, 4*R*)** and **TS-1(3*S*,4*R*)** (2.3 Å) are similar to those observed in asymmetric aldehyde allylboration and allenylboration (~2.2 Å). The lower energy of the (*Z*)-σ-crotylruthenium TS (**TS-1(3*R*,4*R*)**) relative to the (*E*)-σ-crotylruthenium TS (**TS-1(3*S*,4*R*)**) is unexpected as the former TS places the crotyl methyl group axially. However, by doing so, gauche interactions between this group and the aldehyde substituent are minimized as has been found in certain aldol reactions.[34] Furthermore, the crotyl methyl group's proximity to the chiral phosphate also contributes to destabilization of **TS-1(3*S*,4*R*)** (Figure 3). Therefore, the unexpected diastereoselectivity is both a catalyst and a substrate effect.

TS-1(3*R*,4*S*) and **TS-1(3*S*,4*S*)** are destabilized relative to **TS-1(3*R*,4*R*)** and **TS-1(3*S*,4*R*)** due to the absence of the formyl hydrogen bond. **TS-1(3*S*,4*S*)** is further destabilized due to the proximity of the axial methyl group to the chiral phosphate. This leads to the high levels of enantiocontrol observed experimentally. The computed enantioselectivity arising from **TS-1(3*R*,4*R*)** and **TS-1(3*S*,4*S*)** is predicted to be 99 % at 368 K, somewhat higher that seen experimentally (95 %).

The calculated TSs closely resemble the experimental X-ray crystal structure reported for a related catalyst system (Figure 4).[10] To further confirm DFT's ability to model this type of catalyst system, the X-ray crystal structure was optimized starting from the experimental structure (M06/SDD-6-311G(d,p)-IEFPCM(acetone)//B3LYP/SDD-6-31G(d)). Superposition of ruthenium and its 6 surrounding atoms of the calculated and experimental structures led to an RMSD value of 0.08 Å. This shows that computation and experiment are in excellent agreement.

Coordination of the aldehyde to site 2 leads to formyl hydrogen bond lengthening and directional distortion (**TS-2(3*S*,4*S*)** Figure 5). Also, the steric clash between the aldehyde and the aromatic group of the TADDOL framework is much greater in coordination mode 2 than the clash between the σ-crotylruthenium species and the same aromatic group in coordination mode 1 due to the orientation of the chair-like TS ("From above", Figure 5). Both of these factors destabilizes **TS-2(3*S*,4*S*)** relative to **TS-1(3*R*,4*R*)**. Under unoptimized conditions, switching the chiral phosphate's substituent from *m*-xylyl to methyl leads to a drop in enantioselectivity of 77%. Qualitatively, by removing the sterically demanding aromatic substituents, it is expected that coordination of the aldehyde to site 2 becomes comparable to site 1 which would lead to a large drop in ee.

TSs leading to the minor diastereomers via the (*Z*)-σ-crotylruthenium isomer are chair-like with aldehyde substituent axial, or boat-like, and both are higher in energy than **TS-1(3*S*, 4*S*)**. If only the (*Z*)-σ-crotylruthenium isomer were present in solution, higher levels of diastereoselectivity than enantioselectivity would be observed. This is consistent with the very high levels of diastereocontrol observed in aldehyde crotylboration when a single crotylboronate isomer is employed.[35] Our calculations support experimental evidence that shows that rapid isomerization between π-allyl species occurs to form both σ-crotylruthenium isomers.[15–17]

The TS arrangements of aldehyde substituent axial, down and crotyl methyl group equatorial are disfavored relative to **TS-1(3*R*,4*R*)** due to loss of the formyl hydrogen bond and the steric clash of aldehyde substituent with the CO ligand and phosphine in **TS-3(3*R*,4*R*)** and CO and TADDOL-derived scaffold in **TS-3(3*S*,4*S*)** (Figure 6).

BINOL-derived catalyst system

The BINOL-derived scaffold is much longer and more rigid than its TADDOL counterpart (Figure 7). By considering a projection from above, it can be seen that the BINOL-derived phosphate does not intersect the SEGPHOS ligand like the TADDOL-derived phosphate ("From above", Figure 7). Instead, SEGPHOS acts as a steric barrier, restricting rotation of the BINOL-derived ligand. This implies that the chiral nature of SEGPHOS is less important relative to the TADDOL-derived system which may be why BINOL-derived ligands have been found to give excellent levels of enantiocontrol in the absence of a chiral phosphine (Scheme 2).[9]

As before, the π-allyl species are expected to be, or close in energy to, the resting state of the catalytic cycle.[11] The 8 possible π-allyl species once again arise from the following variables: π-crotylruthenium isomer (*syn* or *anti*) and α-methyl group orientation (toward or

away from phosphate, and left or right). For reaction (2) (Scheme 3), DFT calculations show that the thermodynamically preferred π-crotylruthenium isomer is the *syn*-π-allyl species by 7.5 kcal mol^{-1} (Figure 8). However, as described above, these π-allyl species are in rapid equilibrium and that their relative thermodynamic stabilities do not determine diastereocontrol (Curtin-Hammett conditions).[31] Therefore, the kinetics of C-C bond formation were investigated.

The 16 possible chair-like C-C bond forming TSs for reaction (2) once again arise from the following variables: σ-crotylruthenium isomer (*E* or *Z*), aldehyde substituent orientation (toward or away from phosphate, and axial or equatorial) and aldehyde coordination site (site 1 or 2, Scheme 4). All eight chair-like C-C bond forming TSs (aldehyde substituent fixed as equatorial) with an alternative orientation of the C_1-symmetric BINOL-derived ligand were also considered (vide infra, Figure 11). Twenty-nine unique TSs were located in total. The four lowest energy TSs which led to each of the experimentally observed products are shown below in Figure 9 and Table 2.

The lowest energy TS is **TS-4(3*R*,4*S*)** which leads to the major product observed experimentally. From the lowest energy π-allyl species, the barrier to this TS is 23.1 kcal mol^{-1}.

Preferentially, in both most-favored TSs (**TS-4(3*R*,4*S*)** and **TS-4(3*S*,4*S*)**), the formyl hydrogen bond that was observed in reaction (1) is now absent in reaction (2). **TS-4(3*R*,4*R*)** is the lowest energy TS that contains the formyl hydrogen bond, but it is destabilized by 2.5 kcal mol^{-1} relative to **TS-4(3*R*,4*S*)**. The reason for the lack of this interaction upon changing phosphate ligands can be rationalized by considering a projection of the TSs from above (Figure 10). In order to establish this hydrogen-bonding interaction, the chiral phosphate must pivot back toward the phosphine and increase the Ru-O-P angle. When the hydrogen bond is absent, this angle is 139° and 132° in **TS-1(3*R*,4*S*)** and **TS-4(3*R*,4*S*)** respectively. When the hydrogen bond is present, this angle increases to 150° and 144° in **TS-1(3*R*,4*R*)** and **TS-4(3*R*,4*R*)**, respectively. By considering a projection of the TSs from above, looking down on the hydrogen bond, the TADDOL framework can be seen to fit between the steric demands of SEGPHOS and can easily accommodate the increase in Ru-O-P angle ("From above," Figure 10). However, the BINOL framework is orientated directly toward a phenyl group of SEGPHOS making this Ru-O-P angle increase more unfavorable. This catalyst distortion overrides the benefit from the formyl hydrogen bond.

The lack of formyl hydrogen bond in reaction (2), and steric preference for a different TS, explains why nucleophilic attack occurs on the opposite face of the prochiral aldehyde relative to reaction (1). *Syn*-diastereoselectivity is lost as the axial methyl group now points directly toward the phosphate moiety (**TS-4(3*S*,4*S*)**). The lowest energy TS is **TS-4(3*R*,4*S*)** despite the unfavorable gauche interactions between methyl groups. Higher levels of diastereocontrol are observed in the reaction of aromatic aldehydes with a related BINOL-derived catalyst system (Scheme 2).[9] This is because these substrates minimize gauche interactions in the C-C bond forming TS. Furthermore, unlike **TS-1(3*S*,4*R*)**, which is partly destabilized due to the proximity of the crotyl methyl group to the chiral phosphate, this methyl group in **TS-4(3*R*,4*S*)** is directed down, away from the phosphate moiety.

TS-4(3*S*,4*R*), leading to the minor enantiomer, involves coordination of the aldehyde to site 2. This arrangement avoids the formyl hydrogen bond but is destabilized relative to **TS-4(3*R*,4*S*)** due to unfavorable steric interactions with the chiral phosphate. This leads to the high levels of enantiocontrol observed experimentally. The computed enantioselectivity arising from **TS-4(3*R*,4*S*)** and **TS-4(3*S*,4*R*)** was found to be 97 % at 378 K, somewhat higher that seen experimentally (91 %). The lower enantio- and diastereoselectivity observed experimentally for this system relative to the TADDOL-derived catalyst is reproduced by our calculations. Under unoptimized conditions and with an achiral phosphine ligand, switching the chiral phosphate's substituent from mesityl to phenyl leads to a drop in enantioselectivity of 36% (naphthyl methyl group of catalyst replaced by hydrogen in both cases). Qualitatively, by reducing the steric demands of the aromatic substituent, it is expected that coordination of the aldehyde to site 2 becomes comparable to site 1 which would lead to a drop in ee.

Eight chair-like C-C bond forming TSs (aldehyde substituent fixed as equatorial) with an alternative orientation of the C_1-symmetric BINOL-derived ligand were located. The lowest energy TS, **TS-5(3*S*,4*R*)**, of this alternative arrangement was found to be disfavored by 5.3 kcal mol^{-1} relative to **TS-4(3*R*,4*S*)** due to a steric clash between the 2,4,6-trimethylphenyl substituent of the naphthyl ring and a SEGPHOS phenyl group (Figure 11).

4. CONCLUSIONS

DFT calculations show that C-C bond formation in the ruthenium-catalyzed asymmetric hydrohydroxyalkylation of butadiene occurs via a closed-chair Zimmerman-Traxler-type TS. Match/mismatch effects between the chiral phosphate ligand **1b** and the chiral phosphine ligands (*R*)- and (*S*)-SEGPHOS are qualitatively rationalized. Chiral phosphate-dependent stereoselectivity is the result of a hydrogen bond between the phosphoryl oxygen and the aldehyde formyl proton present in TADDOL-derived catalysts, but which is absent in the corresponding BINOL-derived systems due to a steric clash between the chiral phosphine and chiral phosphate ligands.

With this hydrogen bond in place, *syn*-diastereoselectivity with TADDOL-derived catalysts arises from preferential reaction of the (*Z*)-σ-crotylruthenium isomer; this places the crotyl methyl group axially to minimize gauche interactions between this group and the aldehyde (Figure 12).

Because the formyl hydrogen bond cannot be achieved without catalyst distortion in BINOL-derived systems, nucleophilic attack occurs on the opposite face of the prochiral aldehyde. Also, *syn*-diastereoselectivity is lost as the axial methyl group now points directly toward the phosphate moiety. Therefore, the lowest energy TS leads to *anti*-diastereoselectivity despite the unfavorable gauche interactions between methyl groups (Figure 12).

Acknowledgments

We are grateful to The English-Speaking Union (Lindemann Trust Fellowship to M.N.G.) and the NSF (CHE-1361104 to K.N.H.) for financial support. Computational resources were provided by the UCLA Institute for

Digital Research and Education (IDRE) and the Extreme Science and Engineering Discovery Environment (XSEDE), which is supported by the NSF (OCI-1053575).

REFERENCES

1. Yamamoto Y, Asao N. Chem. Rev. 1993; 93:2207–2293.
2. Marek I, Sklute G. Chem. Commun. 2007:1683–1691.
3. Yus M, González-Gómez JC, Foubelo F. Chem. Rev. 2011; 111:7774–7854. [PubMed: 21923136]
4. Yus M, González-Gómez JC, Foubelo F. Chem. Rev. 2013; 113:5595–5698. [PubMed: 23540914]
5. Kennedy JWJ, Hall DG. Angew. Chem. Int. Ed. Engl. 2003; 42:4732–4739. [PubMed: 14562340]
6. Denmark SE, Fu J. Chem. Rev. 2003; 103:2763–2794. [PubMed: 12914480]
7. Brown HC, Bhat KS. J. Am. Chem. Soc. 1986; 108:293–294.
8. Brown HC, Bhat KS. J. Am. Chem. Soc. 1986; 108:5919–5923. [PubMed: 22175350]
9. Zbieg JR, Yamaguchi E, McInturff EL, Krische MJ. Science. 2012; 336:324–327. [PubMed: 22442385]
10. McInturff EL, Yamaguchi E, Krische MJ. J. Am. Chem. Soc. 2012; 134:20628–20631. [PubMed: 23234459]
11. Li H, Wang Z-X. Organometallics. 2012; 31:2066–2077.
12. Xue P, Bi S, Sung HHY, Williams ID, Lin Z, Jia G. Organometallics. 2004; 23:4735–4743.
13. Silva LC, Gomes PT, Veiros LF, Pascu SI, Duarte MT, Namorado S, Ascenso JR, Dias AR. Organometallics. 2006; 25:4391–4403.
14. Zimmerman HE, Traxler MD. J. Am. Chem. Soc. 1957; 79:1920–1923.
15. Chen T-Y, Tsutsumi R, Montgomery TP, Volchkov I, Krische MJ. J. Am. Chem. Soc. 2015; 137:1798–1801. [PubMed: 25642996]
16. Liang T, Nguyen KD, Zhang W, Krische MJ. J. Am. Chem. Soc. 2015; 137:3161–3164. [PubMed: 25734220]
17. Zbieg JR, McInturff EL, Leung JC, Krische MJ. J. Am. Chem. Soc. 2011; 133:1141–1144. [PubMed: 21175178]
18. Frisch, MJ., et al. Gaussian 09. Wallingford, CT: Gaussian, Inc.; 2013.
19. Becke AD. Phys. Rev. A. 1988; 38:3098–3100. [PubMed: 9900728]
20. Lee C, Yang W, Parr RG. Phys. Rev. B. 1988; 37:785–789.
21. Zhao Y, Truhlar D. Theor. Chem. Acc. 2008; 120:215–241.
22. Tomasi J, Mennucci B, Cammi R. Chem. Rev. 2005; 105:2999–3093. [PubMed: 16092826]
23. Simón L, Goodman JM. Org. Biomol. Chem. 2011; 9:689–700. [PubMed: 20976314]
24. Grayson MN, Goodman JM. J. Org. Chem. 2015; 80:2056–2061. [PubMed: 25629214]
25. Overvoorde LM, Grayson MN, Luo Y, Goodman JM. J. Org. Chem. 2015; 80:2634–2640. [PubMed: 25654215]
26. Miyazaki H, Herbert MB, Liu P, Dong X, Xu X, Keitz BK, Ung T, Mkrtumyan G, Houk KN, Grubbs RH. J. Am. Chem. Soc. 2013; 135:5848–5858. [PubMed: 23547887]
27. Yang Y-F, Chung LW, Zhang X, Houk KN, Wu Y-D. J. Org. Chem. 2014; 79:8856–8864. [PubMed: 25157438]
28. Cannon JS, Zou L, Liu P, Lan Y, O'Leary DJ, Houk KN, Grubbs RH. J. Am. Chem. Soc. 2014; 136:6733–6743. [PubMed: 24731019]
29. Legault, CY. CYLView, 1.0b. Sherbrooke, Quebec, Canada: Université de Sherbrooke; 2009. http://www.cylview.org
30. Dugas GJ, Lam Y, Houk KN, Krauss IJ. J. Org. Chem. 2014; 79:4277–4284. [PubMed: 24754566]
31. Seeman JI. Chem. Rev. 1983; 83:83–134.
32. Grayson MN, Pellegrinet SC, Goodman JM. J. Am. Chem. Soc. 2012; 134:2716–2722. [PubMed: 22239113]
33. Grayson MN, Goodman JM. J. Am. Chem. Soc. 2013; 135:6142–6148. [PubMed: 23517191]

34. Lam Y, Houk KN, Scheffler U, Mahrwald R. J. Am. Chem. Soc. 2012; 134:6286–6295. [PubMed: 22458689]

35. Jain P, Antilla JC. J. Am. Chem. Soc. 2010; 132:11884–11886. [PubMed: 20690662]

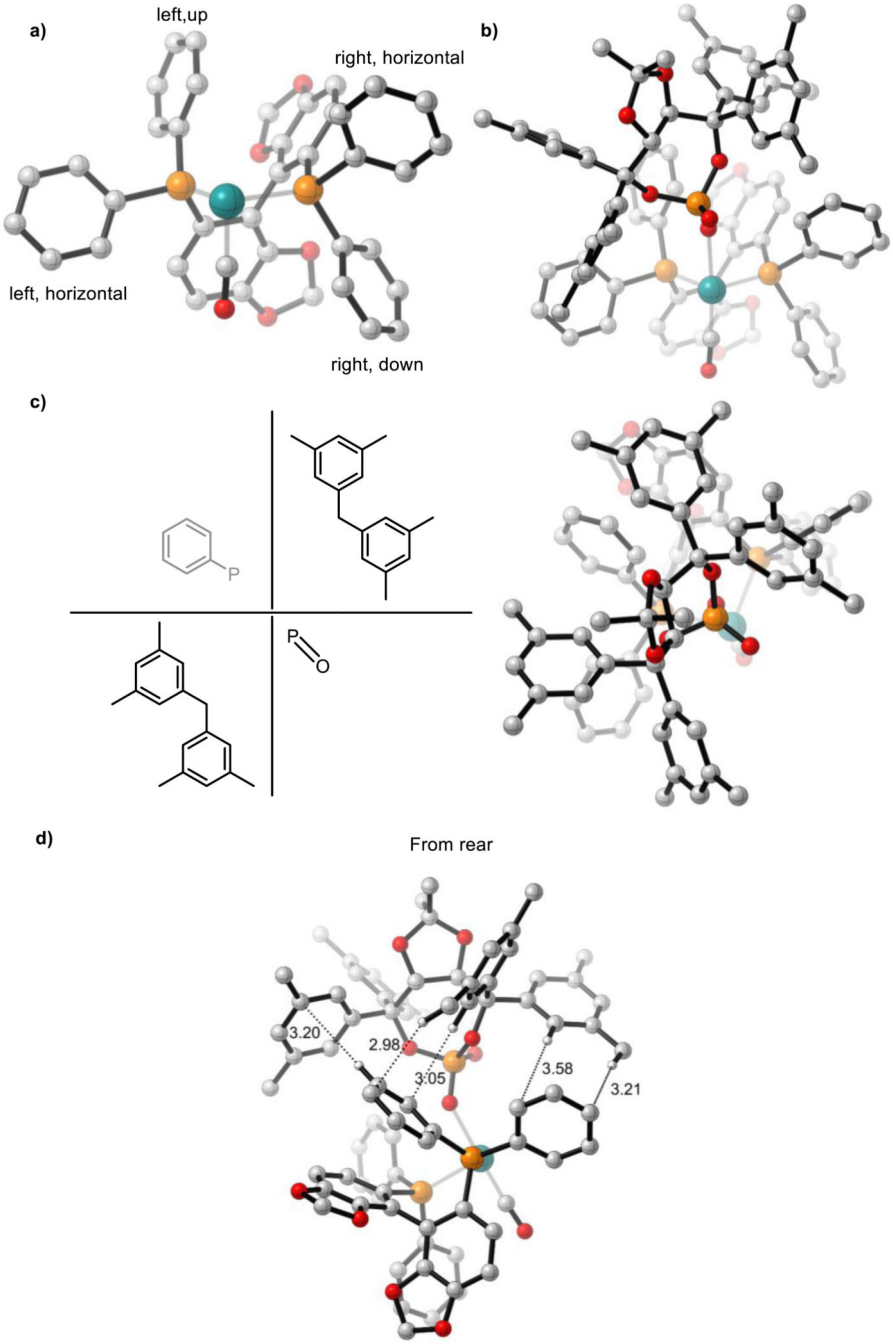

Figure 1.

a, (*S*)-SEGPHOS bound to ruthenium. **b**, TADDOL-derived phosphate and its slanted orientation relative to the P-Ru-P plane. **c**, Catalyst system viewed from above. The catalyst's conformational rigidity is in part due to a SEGPHOS phenyl group which occupies an empty quadrant of the TADDOL-derived scaffold (top-left), preventing phosphate rotation. **d**, Network of CH-π interactions. All structures are derived from optimized *syn*-π-allyl species, non-critical atoms omitted for clarity. M06/SDD-6-311G(d,p)-IEFPCM(acetone)//B3LYP/SDD-6-31G(d).

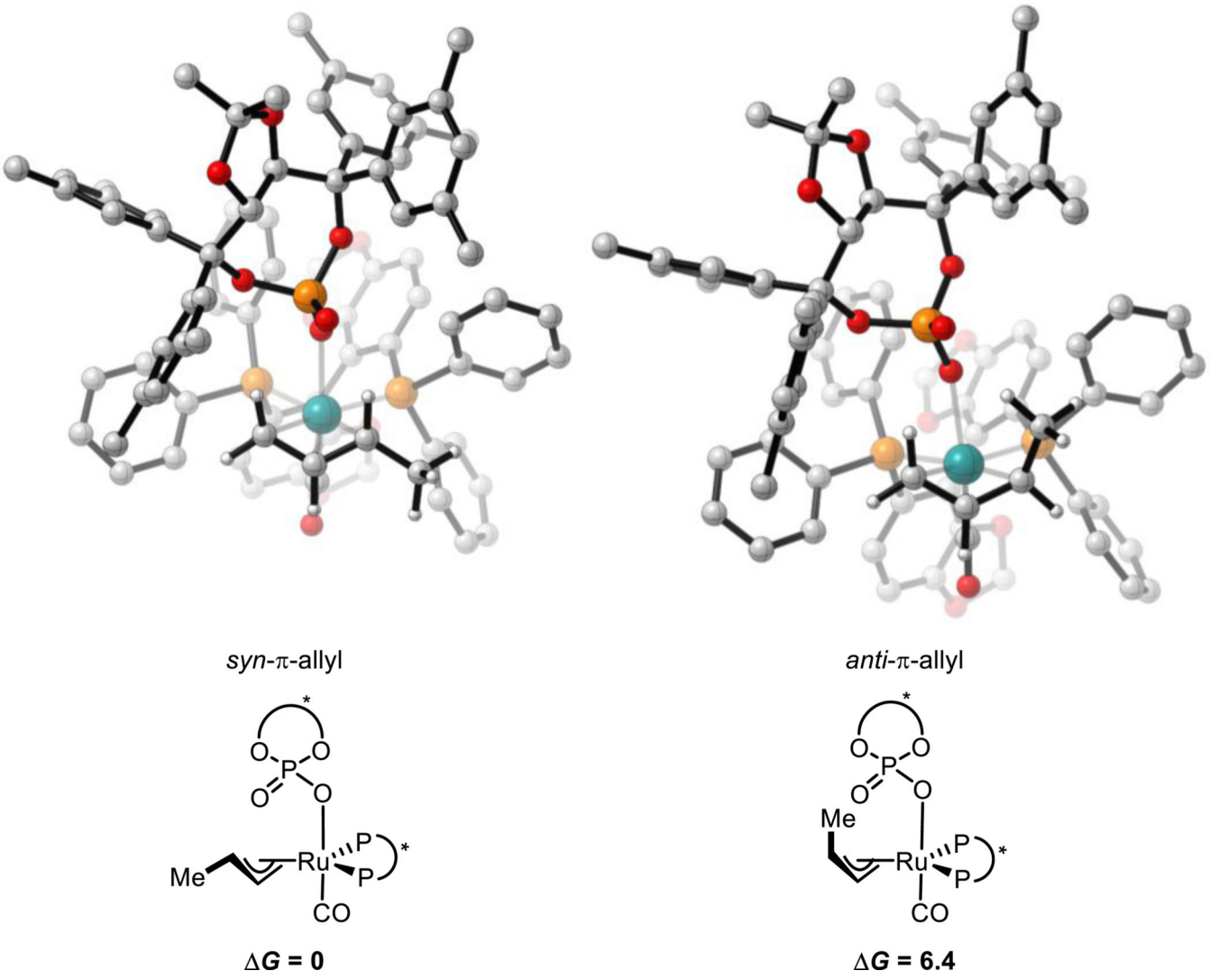

Figure 2.

Lowest energy *syn*- and *anti*-π-crotylruthenium isomers in reaction (1). M06/SDD-6-311G(d,p)-IEFPCM(acetone)//B3LYP/SDD-6-31G(d). Non-critical hydrogen atoms omitted for clarity. X = chiral phosphate. All energies in kcal mol^{-1}.

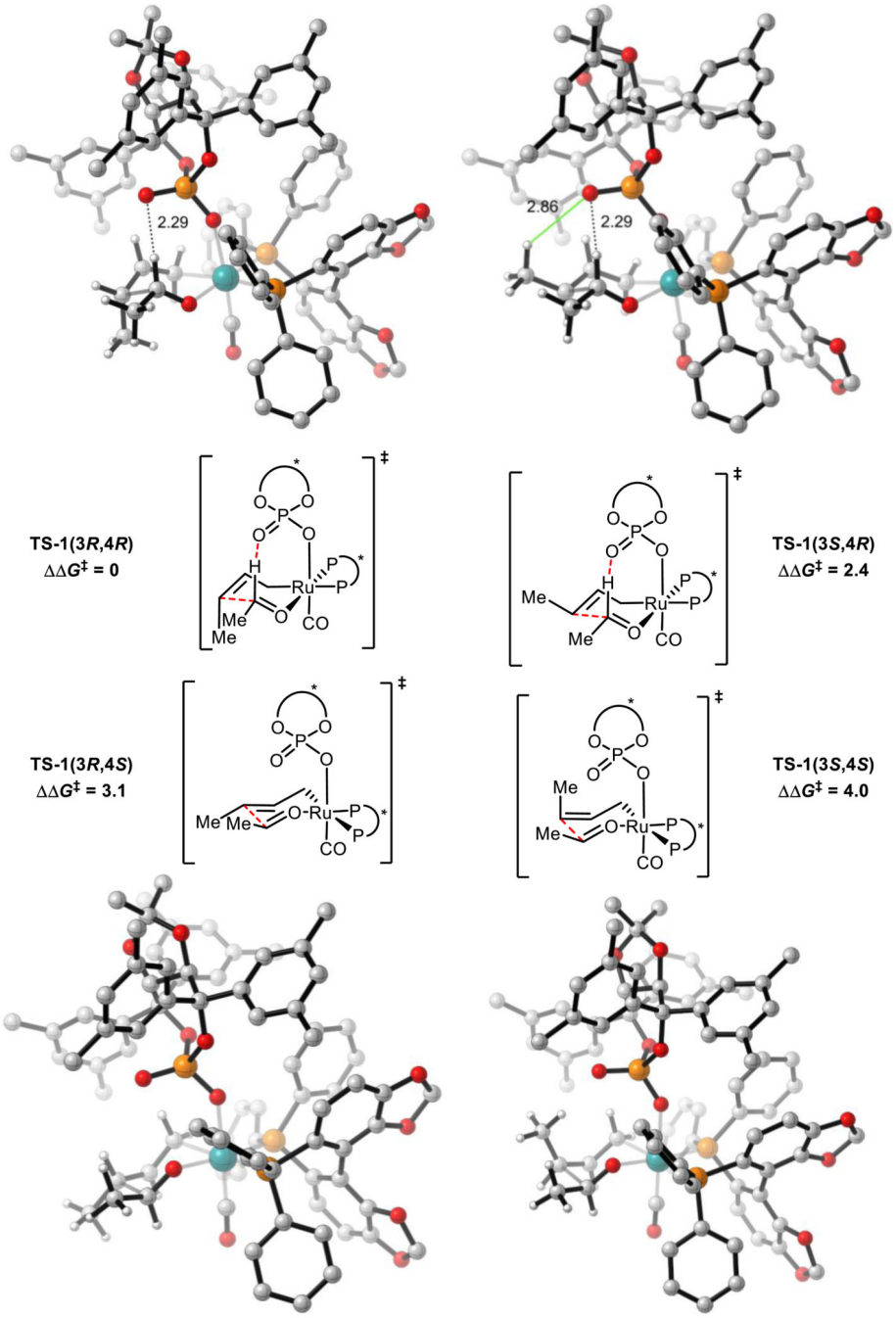

Figure 3.

C-C bond forming TSs for reaction (1). M06/SDD-6-311G(d,p)-IEFPCM(acetone)//B3LYP/SDD-6-31G(d). Non-critical hydrogen atoms omitted for clarity. All energies in kcal mol^{-1}. **TS-1(3*S*,4*R*)** is destabilized relative to **TS-1(3*R*,4*R*)** by a phosphate-substrate steric interaction (green line in **TS-1(3*S*,4*R*)**) and gauche interactions.

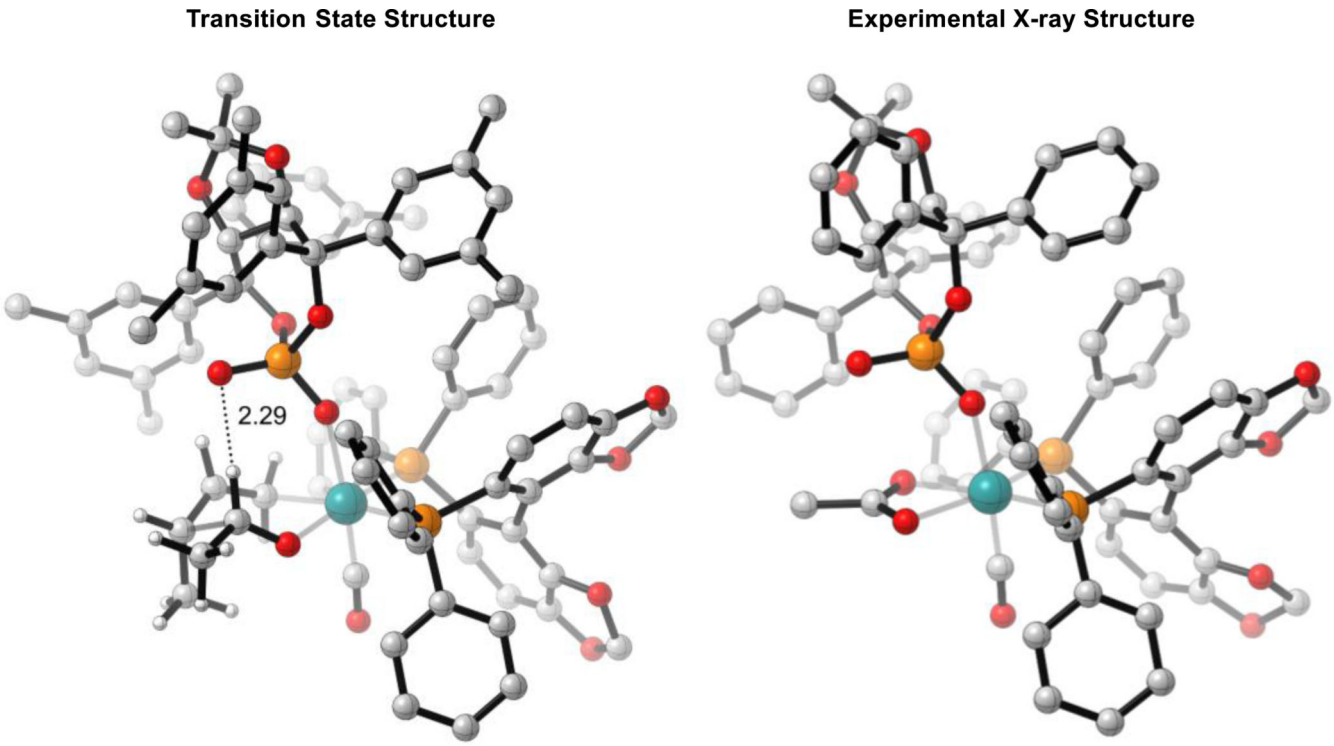

Figure 4.

Comparison of **TS-1(3*R*,4*R*)** and the X-ray crystal structure of a related catalyst system. M06/SDD-6-311G(d,p)-IEFPCM(acetone)//B3LYP/SDD-6-31G(d). Non-critical hydrogen atoms omitted for clarity.

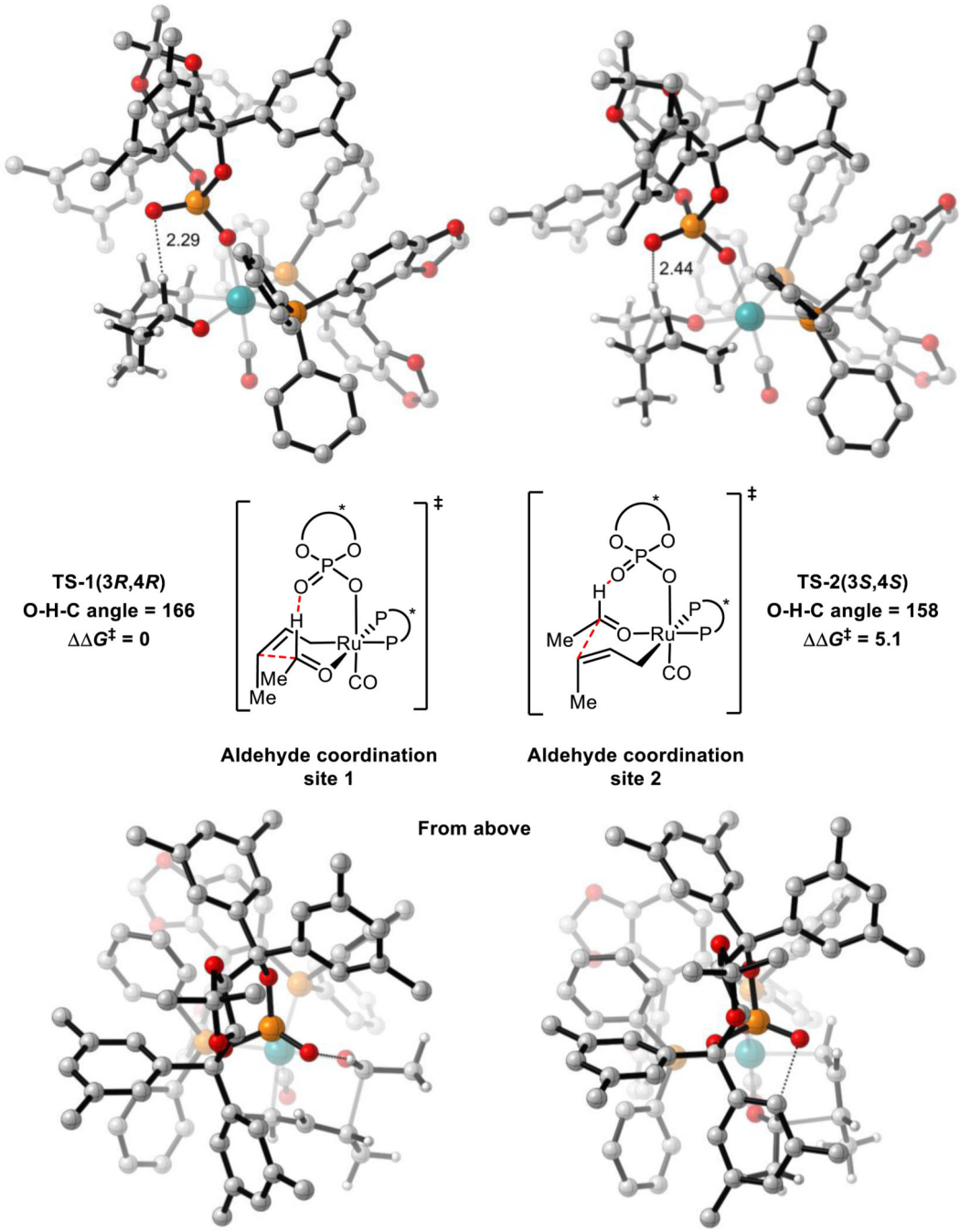

Figure 5.

Comparison of aldehyde coordination sites in C-C bond forming TSs for reaction (1). O-H-C angle defined by P=O oxygen and aldehyde CH. M06/SDD-6-311G(d,p)-IEFPCM(acetone)//B3LYP/SDD-6-31G(d). Non-critical hydrogen atoms omitted for clarity. All energies in kcal mol^{-1}.

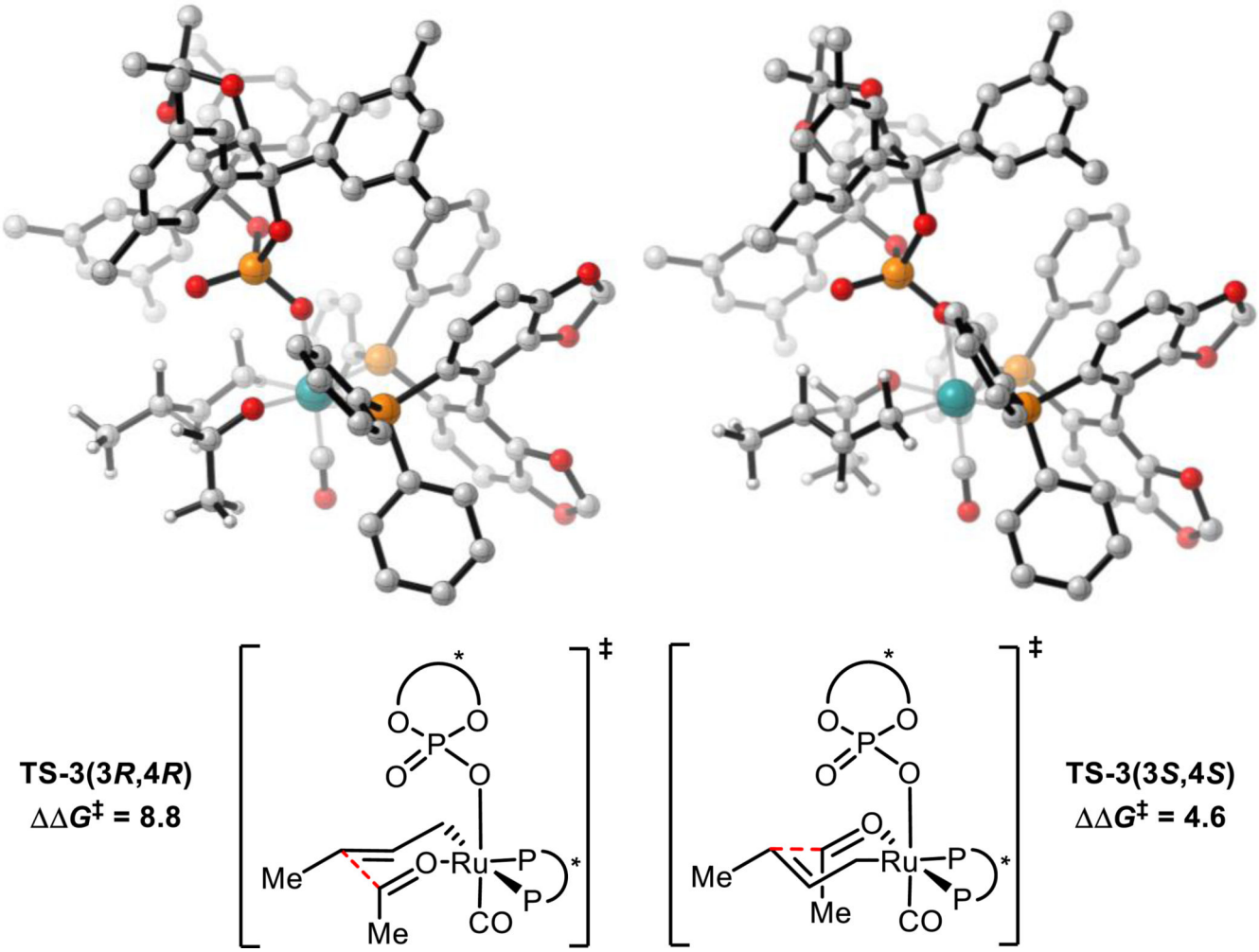

Figure 6.

TS arrangements of aldehyde substituent axial, down and crotyl methyl group equatorial for reaction (1). Free energies relative to **TS-1(3*R*,4*R*)**. M06/SDD-6-311G(d,p)-IEFPCM(acetone)//B3LYP/SDD-6-31G(d). Non-critical hydrogen atoms omitted for clarity. All energies in kcal mol^{-1}.

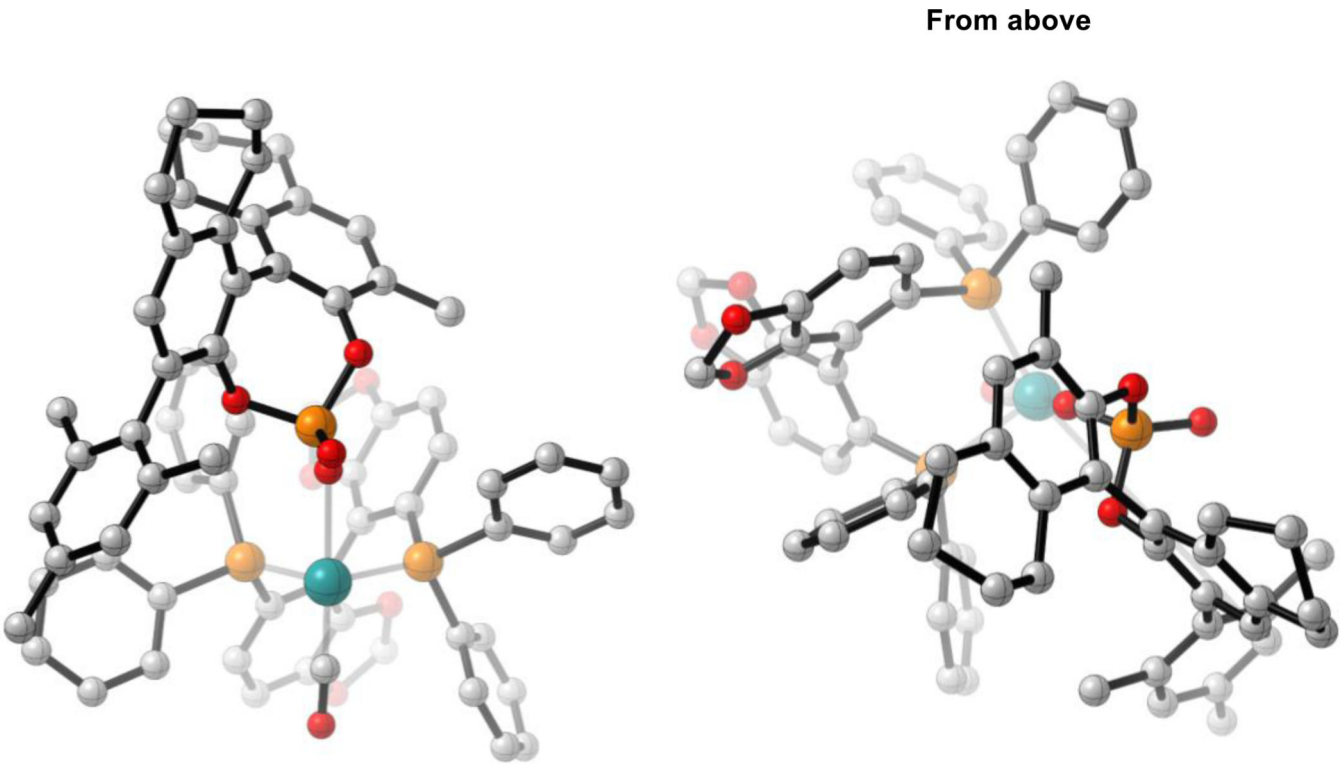

Figure 7.

Different views of the BINOL-derived catalyst system. All structures are derived from optimized *syn*-π-allyl species, non-critical atoms omitted for clarity. M06/SDD-6-311G(d,p)-IEFPCM(acetone)//B3LYP/SDD-6-31G(d).

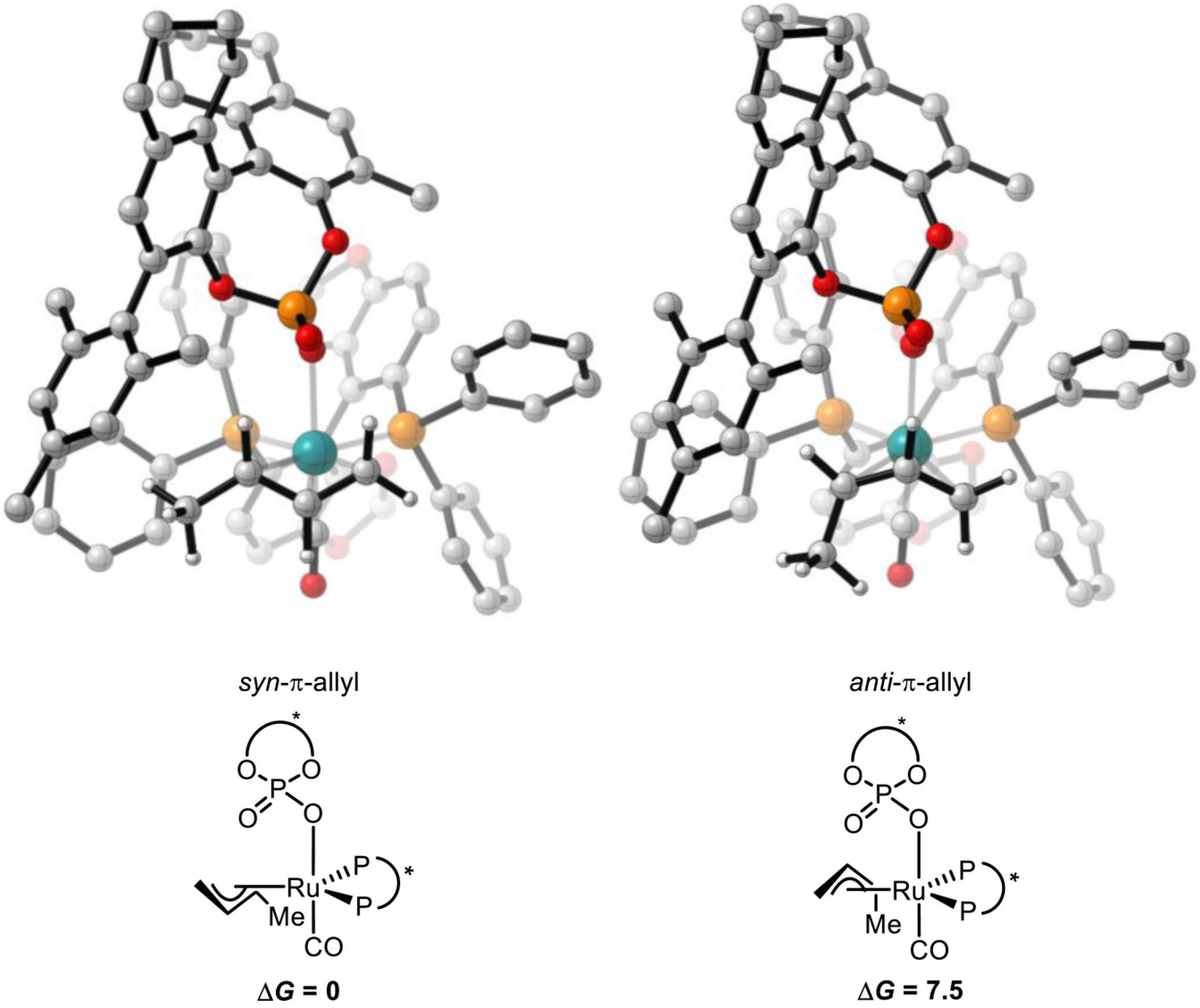

Figure 8.

Lowest energy *syn*- and *anti*-π-crotylruthenium isomers in reaction (2). M06/SDD-6-311G(d,p)-IEFPCM(acetone)//B3LYP/SDD-6-31G(d). Non-critical hydrogen atoms omitted for clarity. X = chiral phosphate. All energies in kcal mol^{-1}.

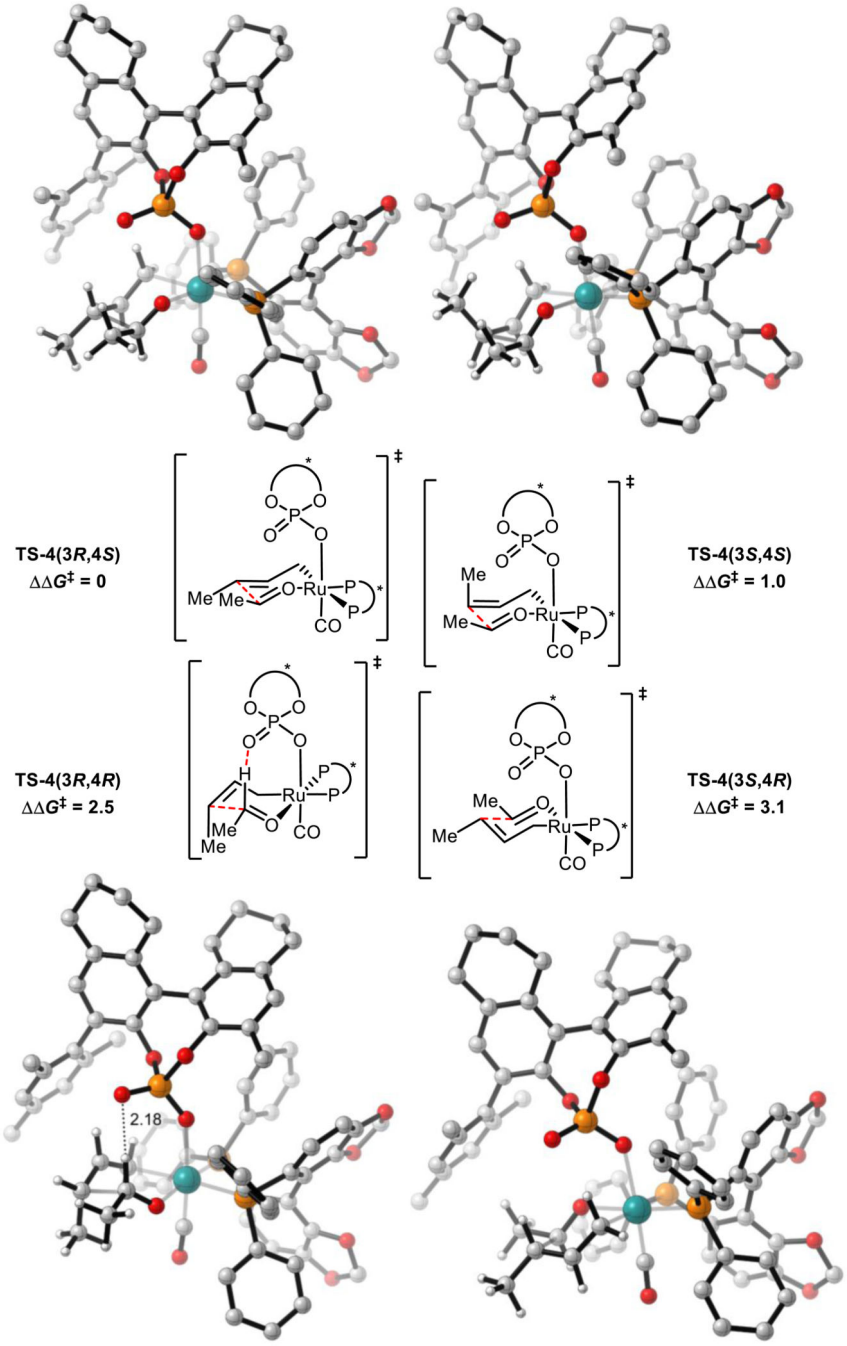

Figure 9.

C-C bond forming TSs for reaction (2). M06/SDD-6-311G(d,p)-IEFPCM(acetone)//B3LYP/SDD-6-31G(d). Non-critical hydrogen atoms omitted for clarity. All energies in kcal mol^{-1}.

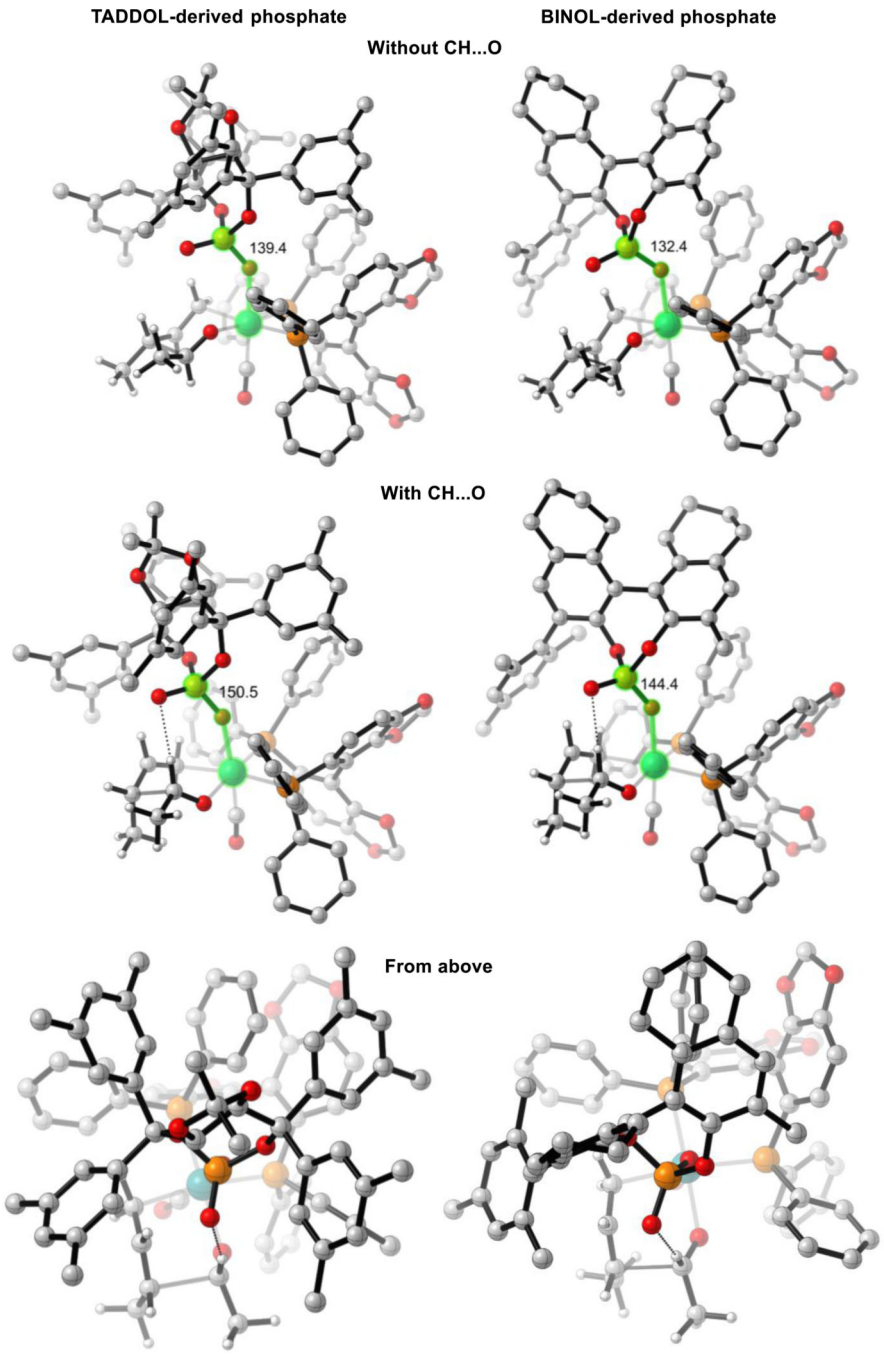

Figure 10.

Comparison of TSs with and without the formyl hydrogen bond. M06/SDD-6-311G(d,p)-IEFPCM(acetone)//B3LYP/SDD-6-31G(d). Measured angle highlighted in green. Non-critical hydrogen atoms omitted for clarity.

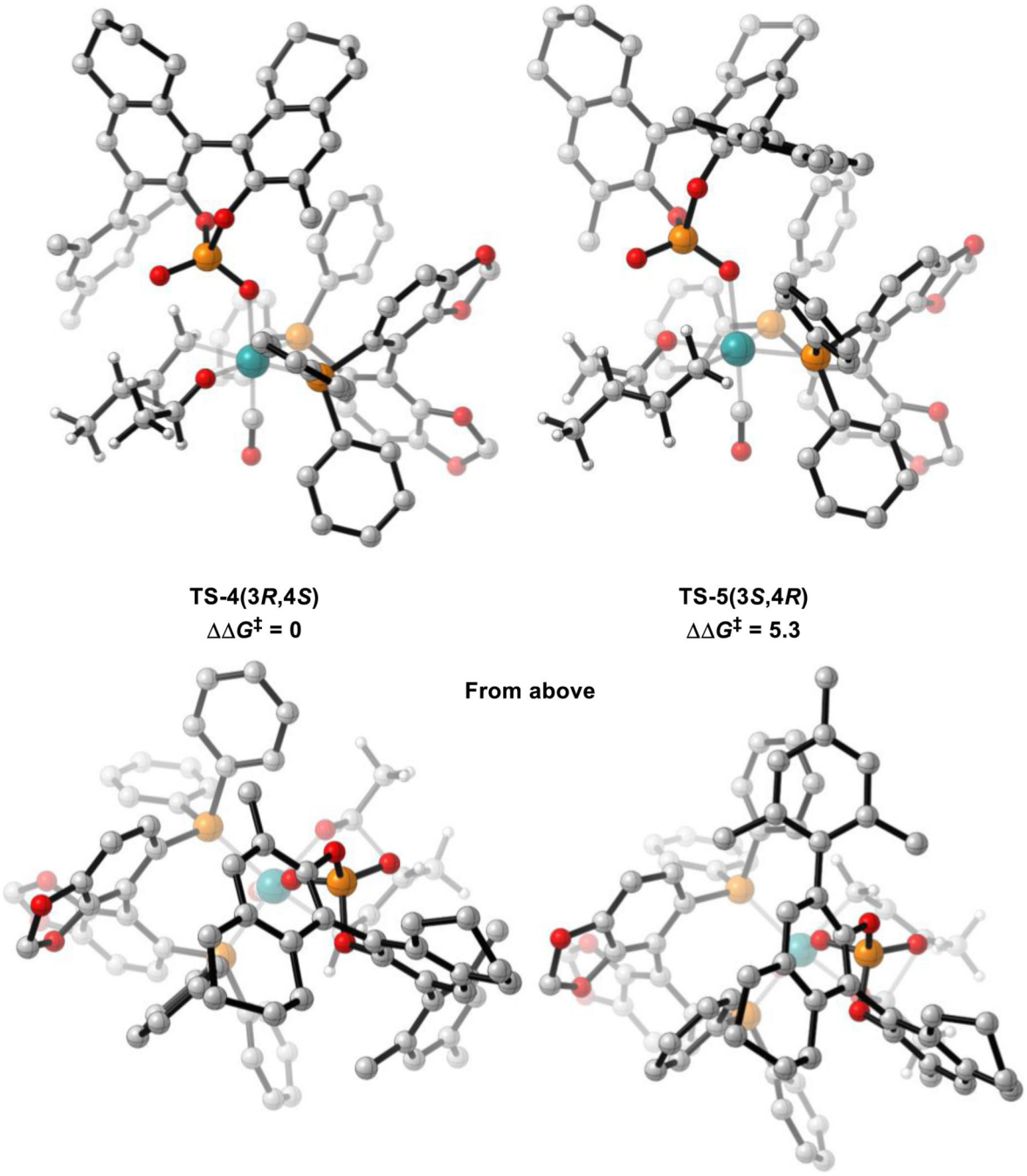

Figure 11.

TSs with different conformations of the C_1-symmetric BINOL-derived ligand. M06/SDD-6-311G(d,p)−IEFPCM(acetone)//B3LYP/SDD-6-31G(d). Non-critical hydrogen atoms omitted for clarity. All energies in kcal mol^{-1}.

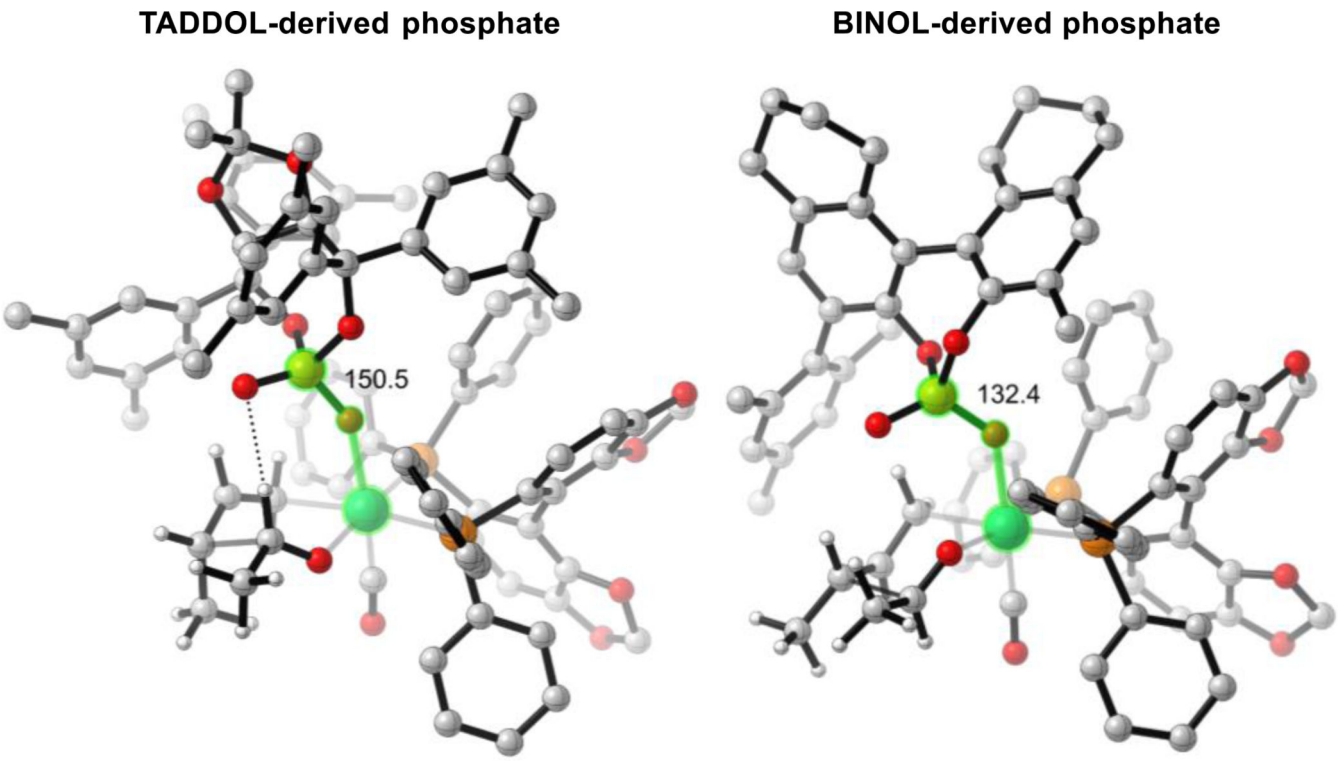

Figure 12.

Lowest energy C-C bond forming TSs for reactions (1) and (2). M06/SDD-6-311G(d,p)-IEFPCM(acetone)//B3LYP/SDD-6-31G(d). Non-critical hydrogen atoms omitted for clarity.

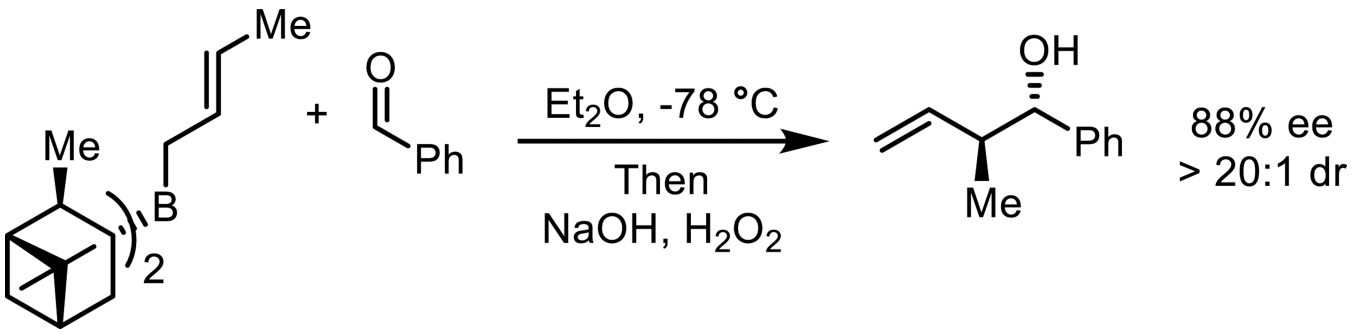

Scheme 1.
Example of reagent-controlled crotylation of carbonyl compounds.[7,8]

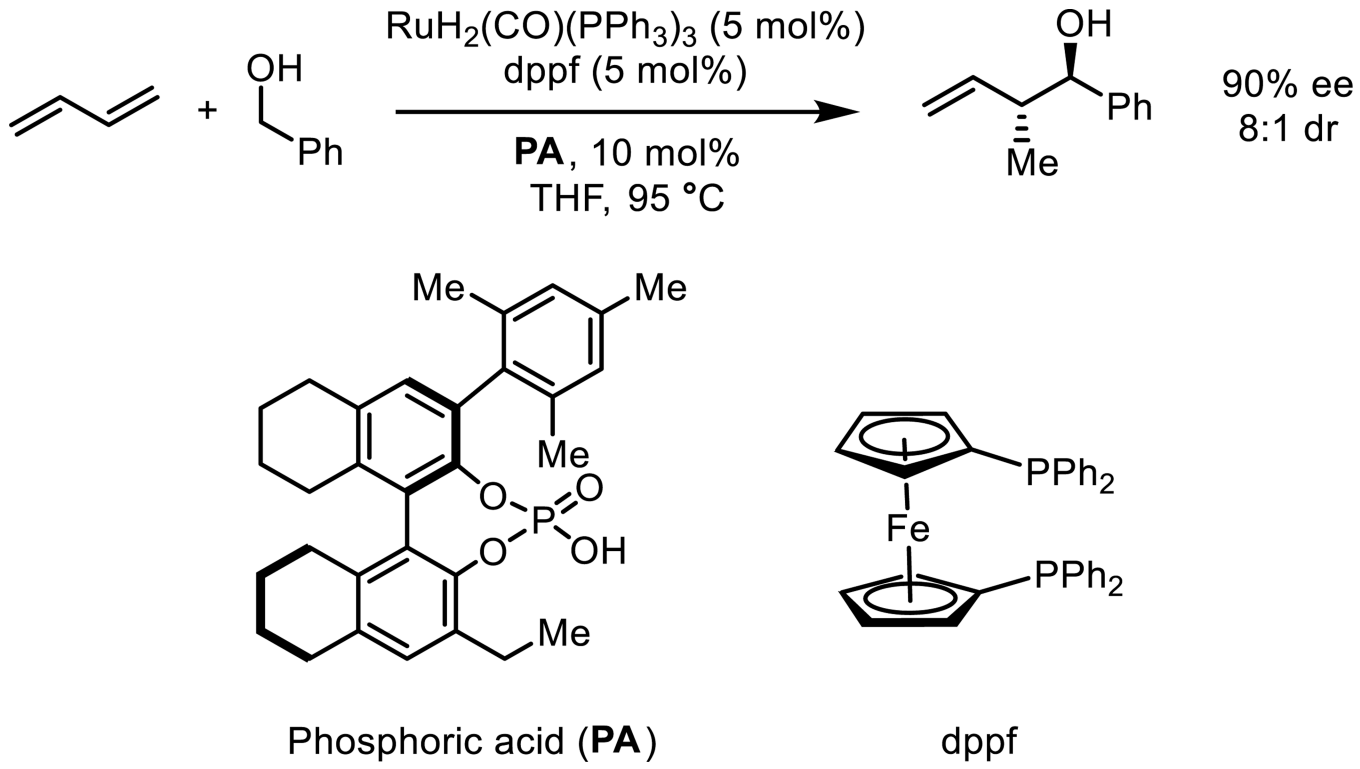

Scheme 2.

The ruthenium-catalyzed diastereo- and enantioselective hydrohydroxyalkylation of butadiene.[9]

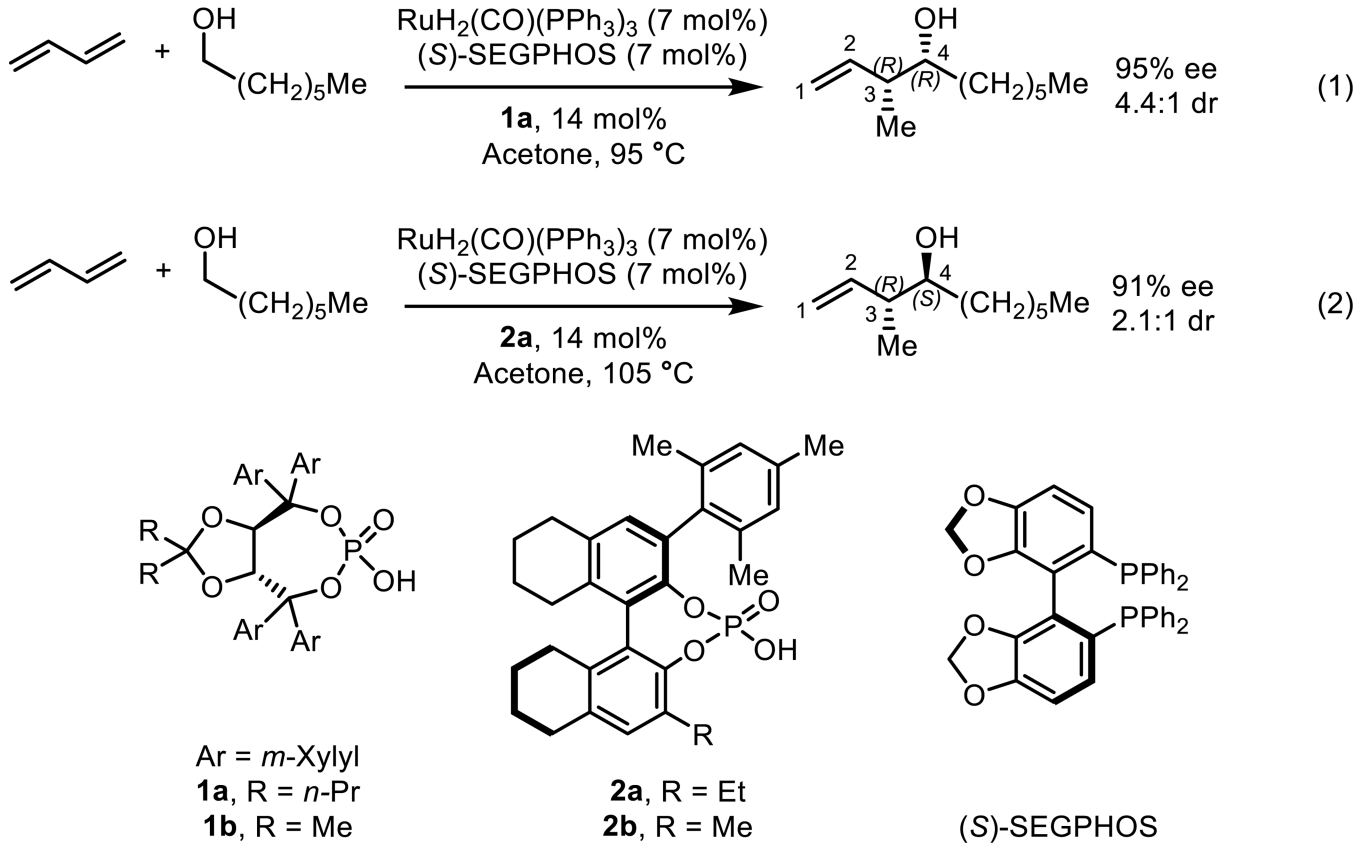

Scheme 3.

Chiral phosphate-dependent stereoselectivity in the ruthenium-catalyzed diastereo- and enantioselective hydrohydroxyalkylation of butadiene.[10]

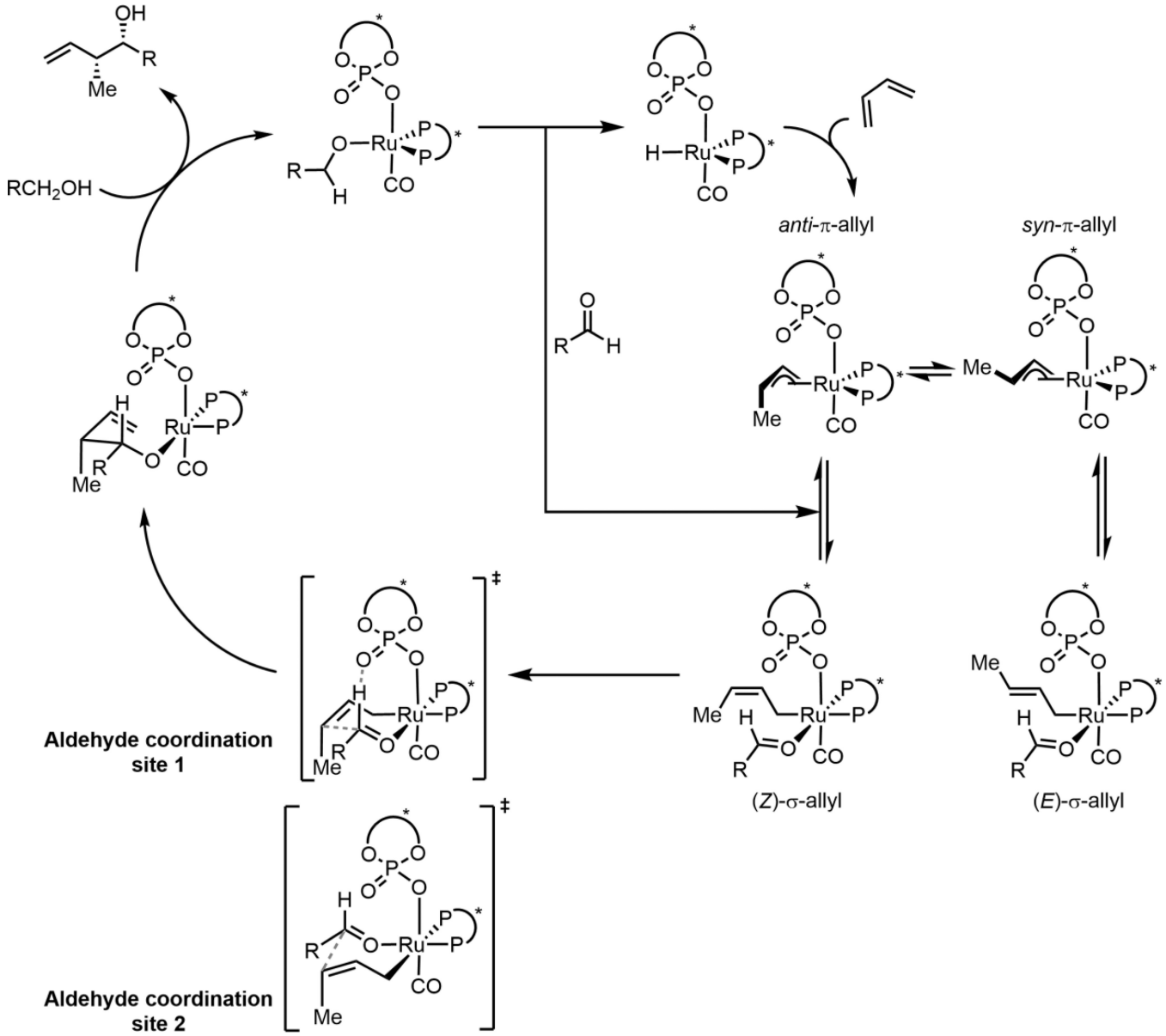

Scheme 4.
Proposed catalytic cycle.[9,10]

Table 1

Comparison of C-C bond forming TSs for reaction (1). (3*R*,4*R*) = major product. See Scheme 4 for aldehyde coordination sites.

	TS	σ-crotylruthenium isomer	Aldehyde R group	Aldehyde coordination site	$\Delta\Delta G^{\ddagger}$ (kcal mol^{-1})	CH…O
TS-1(3*R*,4*R*)	Chair	*Z*	Equatorial	1	0	Yes
TS-1(3*S*,4*R*)	Chair	*E*	Equatorial	1	2.4	Yes
TS-1(3*R*,4*S*)	Chair	*E*	Equatorial	1	3.1	No
TS-1(3*S*,4*S*)	Chair	*Z*	Equatorial	1	4.0	No

Table 2

Comparison of C-C bond forming TSs for reaction (2). (3*R*,4*S*) = major product. See Scheme 4 for aldehyde coordination sites.

	TS	σ-crotylruthenium isomer	Aldehyde R group	Aldehyde coordination site	ΔΔG‡ (kcal mol^{-1})	CH…O
TS-4(3*R*,4*S*)	Chair	*E*	Equatorial	1	0	No
TS-4(3S,4S)	Chair	*Z*	Equatorial	1	1.0	No
TS-4(3*R*,4*R*)	Chair	*Z*	Equatorial	1	2.5	Yes
TS-4(3S,4*R*)	Chair	*E*	Equatorial	2	3.1	No

J Am Chem Soc. Author manuscript; available in PMC 2016 July 15.